Journal of Engineering Mathematics 21: 87–99 (1987)

Wave forces on steeply-sloping sea walls: oblique incidence

W.D. McKEE
School of Mathematics, University of New South Wales, P.O. Box 1, Kensington, N.S.W. 2033, Australia

Received 6 June 1986; accepted in revised form 5 January 1987

Abstract

Previous work, [3], studying the forces exerted by non-breaking, normally-incident water waves of small amplitude on a sloping sea wall is here extended to the case of oblique incidence. The range of applicability of the Galerkin solutions is increased by means of the Shanks transform. Results are presented for a planar, outward-sloping sea wall. In shallow water, the total normal wave force per unit span is found to decrease as the wall slope increases, except for extremely obliquely incident waves. In deep water, it increases. Regarded as a function of the angle of incidence θ, the wave force in shallow water is virtually independent of θ, except for very oblique waves. In deep water, by contrast, the force first increases with θ and then decreases. In this case, the maximum wave force does not occur for normally incident waves.

1. Introduction

In a recent paper in this Journal, Kachoyan and McKee [3] studied the forces exerted by non-breaking, normally-incident water waves on a steeply-sloping planar sea wall using linearised potential theory. They found that, in deep water, the total normal wave force increased as the slope of the wall increased whereas the converse was true in shallow water. In water of intermediate depth, the force was found to be only weakly dependent upon the slope of the wall, at least for the range of wall slopes for which their Galerkin method was valid. This paper extends their work to the case of obliquely incident waves. Both the Galerkin and perturbation methods developed in [3] are readily generalised to cover oblique incidence. However, the perturbation method is found to be invalid for extremely obliquely incident waves and a modified perturbation approach is developed to deal with this situation. Further, it was found in [3] that the Galerkin method became numerically unreliable as the wall became less steep. In this paper, we extend the region of validity of the Galerkin method by the use of the Shanks transform which is an extrapolation technique based on the assumption that the errors in three successive approximations to a quantity form the consecutive terms of a geometric progression.

All the numerical results to be presented in this paper will be for the case of a planar outward-sloping sea wall. The integrals which arise can then all be evaluated analytically. For fixed angle of incidence, the qualitative behaviour of the total normal wave force as a function of the wall slope in both deep and shallow water is found to be broadly similar to that of the normal incidence case except for extremely obliquely incident waves. However, the most interesting and unexpected result obtained in this paper is that, in deep water and with all other parameters fixed, the maximum wave force does not occur for normally incident waves but for waves whose angle of incidence depends on the other parameters of the problem. This surprising result does have some analogues elsewhere in the literature. For example, Fenton [1] studied non-linear waves against a vertical sea wall and found that the maximum force did not occur for normally incident waves.

2. Formulation

As in [3], and employing the same notation and non-dimensionalisation as that paper, we consider small-amplitude water waves in the region bounded by a flat bottom at $y=-1$, a free surface at $y=0$ and a sea wall $x=f(y)$ where $f(0)=0$. A monochromatic wave train of frequency ω is assumed to be incident from $x=\infty$ with angle of incidence θ and to be perfectly reflected from the wall, thus forming a pattern of short-crested waves far from the wall. The geometry is shown in Fig. 1. Hence in non-dimensional variables we have to solve

$$\frac{\partial^2\Phi}{\partial x^2}+\frac{\partial^2\Phi}{\partial y^2}-m^2\Phi=0 \quad \text{for } -1<y<0 \quad \text{and } f(y)<x<\infty, \tag{1}$$

$$\frac{\partial\Phi}{\partial y}=0 \quad \text{at } y=-1 \quad \text{for } x>f(-1), \tag{2}$$

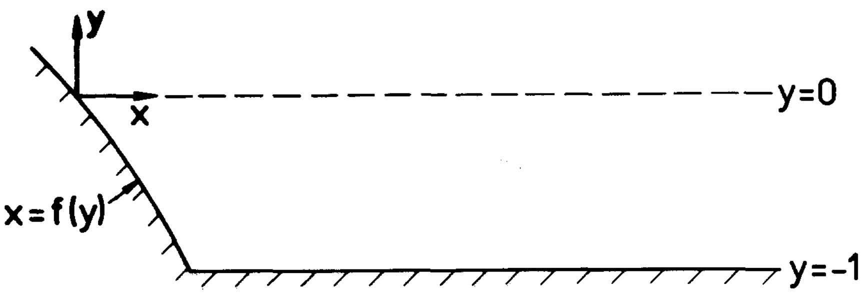

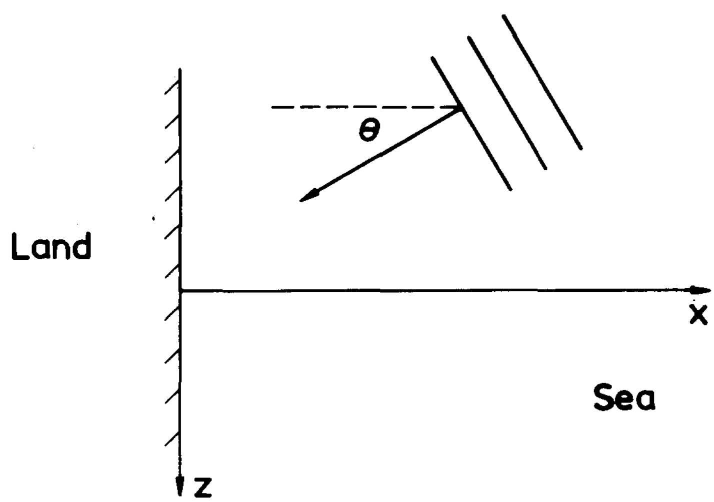

Fig. 1a. An elevation view showing the sea wall. In all computations, the equation of the wall is taken to be $x=-\alpha y$ and hence the wall is a plane inclined at an angle $\tan^{-1}\alpha$ to the negative y axis.

Fig. 1b. A plan view showing the waves incident upon the sea wall with angle of incidence θ. For normally-incident waves, $\theta=0$.

$$\frac{\partial \Phi}{\partial y} = \omega^2 \Phi \quad \text{at } y = 0 \quad \text{for } x > 0, \tag{3}$$

$$\frac{\partial \Phi}{\partial x} - f'(y)\frac{\partial \Phi}{\partial y} = 0 \quad \text{on } x = f(y) \quad \text{for } -1 < y < 0, \tag{4}$$

subject to

$$\Phi \sim \operatorname{sech} k \cosh k(1+y) \cos(lx + \beta) \quad \text{as } x \to \infty. \tag{5}$$

In the above, k is the unique positive root of $\omega^2 = k \tanh k$, $l = k \cos \theta$, $m = k \sin \theta$ and the velocity potential ϕ is

$$\phi(x, y, z, t) = \Phi(x, y) \cos(mz - \omega t).$$

The phase β, which is zero for a vertical plane wall $x = 0$, has to be determined as part of the problem. The quantity of primary interest is the wave force per unit span $\mathbf{F}$ given by

$$\mathbf{F} = \sin(mz - \omega t) \int_{-1}^{0} (\mathbf{i} - \mathbf{j} f'(y)) \Phi(f(y), y)\, \mathrm{d}y. \tag{6}$$

For a vertical plane wall,

$$\mathbf{F} = k^{-1} \tanh k \mathbf{i} \sin(mz - \omega t).$$

In all the figures in this paper, we will scale the forces by $k^{-1} \tanh k$ so that, with the $\sin(mz - \omega t)$ factor omitted, the force is unity for a vertical planar wall. The magnitude of the total normal wave force per unit span scaled in this way will be denoted by G and its horizontal component by H. The quantity $k^{-1} \tanh k$ was shown as a function of frequency in Fig. 6 of [3].

Using separation of variables, we may write down a solution of (1) which satisfies all the conditions of the problem except (4) as

$$\Phi = \operatorname{sech} k \left\{ \psi_0(y) \cos(lx + \beta) + \sum_{n=1}^{\infty} A_n \psi_n(y) \exp(-P_n x) \right\}, \tag{7}$$

where

$$\psi_0(y) = \cosh k(1+y)$$

and

$$\psi_n(y) = \cos \kappa_n (1+y) \quad \text{for } n = 1, 2, 3, \ldots.$$

Here, κ_n (where $(n - \frac{1}{2})\pi < \kappa_n < n\pi$) is the nth positive root of $\omega^2 = -\kappa_n \tan \kappa_n$ and $P_n = (\kappa_n^2 + m^2)^{1/2}$. Our task is then to find β and the A_n such that (4) is satisfied. The force is then found from (6).

3. Perturbation and Galerkin solutions

We consider first a steep wall $x = \alpha g(y)$ where $|\alpha| \ll 1$ and g is an O(1) function with $g(0) = 0$. Since β and the A_n are all zero when $\alpha = 0$ it is natural to seek a regular perturbation expansion of the form

$$\beta = \sum_{j=1}^{\infty} \beta_j \alpha^j; \quad A_n = \sum_{j=1}^{\infty} A_{nj} \alpha^j. \tag{8}$$

Following the same steps as outlined in [3] for $m = 0$, we transfer the boundary condition (4) at $x = \alpha g(y)$ to $x = 0$ by means of a Taylor series in x. Collecting up the coefficients of like powers of α and invoking the orthogonality of the eigenfunctions ψ_0, ψ_1, ψ_2, ... we find

$$\beta_1 = \frac{4\int_{-1}^{0} g(y)\left\{m^2(\psi_0(y))^2 + (\psi_0'(y))^2\right\} \mathrm{d}y}{\cos\theta(2k + \sinh 2k)} \tag{9}$$

and

$$A_{n1} = \frac{4\kappa_n \int_{-1}^{0} g(y)\left\{m^2\psi_0(y)\psi_n(y) + \psi_0'(y)\psi_n'(y)\right\} \mathrm{d}y}{P_n(2\kappa_n + \sin 2\kappa_n)}$$

from the O(α) terms and

$$\beta_2 = \frac{4\sum_{j=1}^{\infty} A_{j1} \int_{-1}^{0} g(y)\psi_0(y)\left\{m^2\psi_j(y) + k\psi_j'(y)\right\} \mathrm{d}y}{k\cos\theta(2k + \sinh 2k)} \tag{10}$$

and

$$A_{n2} = \frac{4\kappa_n \sum_{j=1}^{\infty} A_{j1} \int_{-1}^{0} g(y)\left\{m^2\psi_n(y)\psi_j(y) + \psi_n'(y)\psi_j'(y)\right\} \mathrm{d}y}{P_n(2\kappa_n + \sin 2\kappa_n)}$$

from the O(α^2) terms. (A typographical error in the expression for A_{n2} given in [3] when $m = 0$ is here corrected.) From these, the wave force correct to first and second order in α may readily be found. To find the first-order force, one needs only the A_{n1} whereas β_1 and the A_{n2} are also needed to find the force correct to O(α^2).

Similarly, the Galerkin solution of [3] may be generalised by rewriting (7) as

$$\Phi = \operatorname{sech} k\left(1 + B_0^2\right)^{-1/2}\left\{(\cos lx + B_0 \sin lx)\psi_0(y) + \sum_{j=1}^{\infty} B_j\psi_j(y)\exp(-P_j x)\right\}. \tag{11}$$

Substituting this into (4), multiplying by $\psi_i(y)$ for $i = 0, 1, \ldots, N$, integrating from -1 to 0 and truncating at $j = N$ gives a set of $(N + 1)$ simultaneous linear equations for $B_0, B_1, \ldots, B_N$. From the solution of this set, the force may be found using (11) and (6). However, as discussed in [3], the system of linear equations becomes ill-conditioned for large N. Even when the system is not particularly badly ill-conditioned, the estimates of the forces tend to exhibit oscillations with increasing N which become worse as ω and/or α increase. Indeed, the process often seems to be undergoing an oscillatory divergence as N increases. These oscillations can be reduced or even eliminated by means of the Shanks transform discussed by, for example, Van Dyke [4]. In fact, the Shanks transform was implemented in the mathematically equivalent but

Table 1. Shanks table for the scaled total normal wave force G when $\omega = 0.1$, $\alpha = 1.25$ and $\theta = 0°$. The process is described in the text.

1.596596				
1.601138	1.599874			
1.599386	1.600507	1.600433		
1.602494	1.600423	1.600490	1.600380	
1.596288	1.600771	1.600611	1.601782	1.601148
1.612435	1.600474	1.600720	1.600623	
1.566289	1.601900	1.599896		
1.722279	1.606851			
1.278372				
1.278372				
1.606851	1.600040			
1.599896	1.600554	1.599855		
1.600623	1.602498			
1.601148				
1.601148				
1.602498	1.601604			
1.599855				

numerically preferable form of Aitken's Δ^2-process (see, for example, Johnson and Riess [2]).

We show in Table 1 the results for a quite badly behaved case $\omega = 0.1$, $\alpha = 1.25$ and $\theta = 0°$. All calculations were done in double precision FORTRAN on a VAX 11/780. This gives about 16 decimal digits but we only present here the final results rounded to 6 decimal digits. The first column of the upper panel of this table shows the total normal wave force G as estimated from (6) using $N = 0, 1, 2, \ldots, 8$ evanescent modes in the expansion (11). The second column of the upper panel shows the values of G obtained by applying the Shanks transform to the first column, the third column shows the results of applying it to the second column and so on. The middle panel repeats the process taking for its initial values the final values in each of the five columns of the upper panel. The lower panel is derived from the middle panel in a similar manner. The diverging oscillations in the primary estimates shown in the first column of the upper panel are quite clear, as is their elimination by the Shanks transform. From this table,

Table 2. Shanks table for the scaled total normal force G when $\omega = 2.0$, $\alpha = 0.25$ and $\theta = 45°$.

0.9305114				
0.8724722	0.8696426			
0.8697742	0.8696530	0.8696513		
0.8696582	0.8696509	0.8696524	0.8696514	
0.8696513	0.8696560	0.8696426	0.8696495	0.8696511
0.8696656	0.8696642	0.8696657	0.8696640	
0.8696640	0.8696654	0.8696639		
0.8696756	0.8696716			
0.8696696				
0.8696696				
0.8696716	0.8696700			
0.8696639	0.8696640	0.8696639		
0.8696640	0.8696639			
0.8696511				
0.8696511				
0.8696639	0.8696639			
0.8696639				

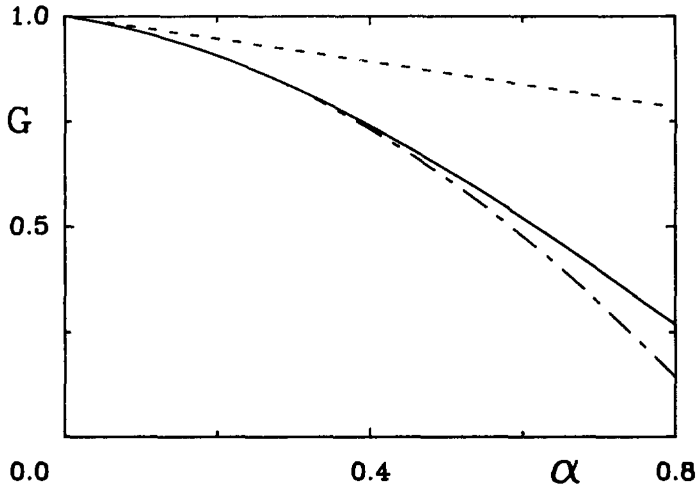

Fig. 2. The scaled, non-dimensional total normal wave force per unit span, G, for a planar, outward sloping sea wall $x = -\alpha y$ when $\omega = 2.0$ and $\theta = 45°$. The scaling factor k^{-1} tanh k by which the results have been divided has the value 0.24967. Shown are the results of the first (- - - - - -) and second (- — - — -) order regular perturbation theories and those of the Shanks-transformed Galerkin method (———).

one would conclude that a value between 1.5999 and 1.6025 was probably correct. Such accuracy is more than enough for graphical purposes and compares well with the value of 1.600764 predicted by shallow-water theory (see [3]). Interestingly, using $N = 1$ or 2 gives quite good results in this case although this was found not to be so in other cases, especially for larger values of ω where the influence of the evanescent modes is greater. A somewhat better behaved example, $\omega = 2$, $\alpha = 0.25$ and $\theta = 45°$ is shown in Table 2. Here one would probably conclude a value of 0.86965 or 0.86966.

The Shanks transform and similar devices are often used nowadays to improve convergence but should always be viewed with a little skepticism since they can sometimes go catastrophically wrong. Nevertheless, when applied to this problem, the Shanks transform has enabled us to extend the range of validity of the Galerkin solutions to larger values of α than was possible in [3]. Eventually, however, when α gets sufficiently large the results become unreliable since the primary estimates are badly affected by the basic ill-conditioning of the system. Simple pairwise averaging was also tried but did not produce results as consistent as those from the Shanks transform.

For waves with small or moderate angles of incidence, numerical comparisons of the results of the first- and second-order perturbation calculations and the Galerkin method are broadly similar to the normal incidence case presented in [3]. That is, the three merge as $\alpha \to 0$ with the second order generally agreeing better with the Galerkin as α increases. A typical example is shown in Fig. 2 for $\omega = 2.0$, $\theta = 45°$ and $0 \leqslant \alpha \leqslant 0.8$. This latter value of α was about the largest for which the Shanks-transformed Galerkin results were reliable. As θ increases, for fixed ω and α, the agreement generally gets worse as suggested by the expressions (9) and (10) for β_1 and β_2 which indicate that the effective expansion parameter may be $\alpha/\cos\theta$ rather than α itself.

4. Very oblique waves

As $\theta \to \pi/2$, (9) and (10) become unbounded and so the perturbation analysis of the previous section breaks down because $\alpha\beta_1$ and $\alpha^2\beta_2$ are no longer small for $\alpha \neq 0$. The first-order forces depend on the A_{n1} and are not divergent, merely inaccurate, as $\theta \to \pi/2$. The second-order forces depend also on the A_{n2} and β_1 and are actually divergent as $\theta \to \pi/2$. The results of the Galerkin method for a plane wall $x = -\alpha y$ indicate that, for fixed ω and $\alpha > 0$, $B_0 \to -\infty$ as $\theta \to \pi/2$. This implies that $\beta \to \pi/2$. Further, the B_n for $n > 0$ all tend to zero as $\theta \to \pi/2$ and so the force tends to zero. There are no numerical difficulties with the Galerkin method for very oblique waves and the obvious reformulation of the surface wave term in (11) as $(\sin lx + B_0 \cos lx)$ gave $B_0 \to 0$ as $\theta \to \pi/2$ for fixed ω and $\alpha > 0$ and force values identical to 5 or 6 decimal places with those obtained from (11) even though a slightly different set of linear equations had to be solved to find the coefficients.

We thus have the situation that the regular perturbation expansion (8) is invalid as $\theta \to \pi/2$ and that for a plane wall $x = -\alpha y$ the Galerkin results predict that, for fixed $\theta \neq \pi/2$, the scaled total normal wave force, G, tends to 1 as $\alpha \downarrow 0$ whereas for fixed $\alpha > 0$ it tends to 0 as $\theta \to \pi/2$. A simple perturbation calculation appropriate for very oblique waves which has the correct limiting behaviour may be constructed as follows. We suppose the wall to be $x = \alpha g(y)$ where $\alpha \neq 0$ and write $l = \sigma\alpha$ where σ is formally assumed to be O(1) with respect to α. The expansions (8) are replaced by

$$\beta = \sum_{j=0}^{\infty} \gamma_j \alpha^j; \quad A_n = \sum_{j=1}^{\infty} \Gamma_{nj} \alpha^j. \tag{12}$$

The leading term in the expansion of β is therefore assumed to be independent of α. The boundary condition (4) is transferred to $x = 0$ by means of a Taylor series in x. Substituting (7) and (12) into this and collecting up the coefficients of like powers of α gives

$$\sigma\psi_0(y) \sin\gamma_0 + g'(y)\psi_0'(y) \cos\gamma_0 + \sum_{n=1}^{\infty} \Gamma_{n1} P_n \psi_n(y) = 0$$

for $-1 < y < 0$ from the $O(\alpha)$ terms and

$$\gamma_1\{g'(y)\psi_0'(y) \sin\gamma_0 - \sigma\psi_0(y) \cos\gamma_0\}$$
$$+ g(y) \sum_{n=1}^{\infty} \Gamma_{n1} P_n^2 \psi_n(y) - \sum_{n=1}^{\infty} \Gamma_{n2} P_n \psi_n(y) = 0$$

for $-1 < y < 0$ from the $O(\alpha^2)$ terms. Multiplying each of these by $\psi_0(y)$ and integrating from -1 to 0, using the orthogonality of the eigenfunctions, gives expressions for γ_0 and γ_1. Similarly, Γ_{n1} and Γ_{n2} are found using ψ_n. For the case $g(y) = -y$ we find

$$\tan\gamma_0 = \frac{k(\cosh 2k - 1)}{\sigma(2k + \sinh 2k)}, \tag{13}$$

$$\Gamma_{n1} = \frac{4k\kappa_n \cos\gamma_0 \{k(\cosh k \cos\kappa_n - 1) + \kappa_n \sinh k \sin\kappa_n\}}{P_n(k^2 + \kappa_n^2)(2\kappa_n + \sin 2\kappa_n)} \tag{14}$$

and

$$\gamma_1 = \frac{4 \sin\gamma_0}{\cosh 2k - 1} \sum_{n=1}^{\infty} \Gamma_{n1} P_n^2 I_n \tag{15}$$

where

$$I_n = \frac{(k^2 - \kappa_n^2)(\cosh k \cos\kappa_n - 1) + 2k\kappa_n \sinh k \sin\kappa_n}{(k^2 + \kappa_n^2)^2}.$$

The wave force per unit span is found to be

$$\mathbf{F} = \frac{\tanh k}{k}(G_0 + \alpha G_1 + O(\alpha^2))\mathbf{n} \sin(mz - \omega t), \tag{16}$$

where $G_0 = \cos \gamma_0$,

$$G_1 = \frac{k}{\sinh k} \sum_{n=1}^{\infty} \Gamma_{n1} \frac{\sin \kappa_n}{\kappa_n} - \gamma_1 \sin \gamma_0$$

and $\mathbf{n}$ is the unit outward normal to the wall.

The behaviour as $\theta \to \pi/2$ can now readily be deduced from these expressions. Firstly, if α is fixed and positive then $\sigma \downarrow 0$ as $\theta \to \pi/2$. Thus $\gamma_0 \to \pi/2$ from (13), $\Gamma_{n1} \to 0$ from (14) and hence $\gamma_1 \to 0$ from (14) and (15). Hence $G \to 0$, in accordance with the numerical findings of the Galerkin method. Secondly, if $\alpha \downarrow 0$ for fixed $\theta \neq \pi/2$, $\sigma \to \infty$ and so γ_0 and γ_1 both tend to zero. Thus, when the $(k^{-1} \tanh k) \sin(mz - \omega t)$ factor is suppressed, the force per unit span tends to unity in this limit. Numerical results are depicted in Fig. 3 for $\omega = 2.0$ and $\alpha = 0.25$ where we show the magnitude, G, of the scaled total normal wave force per unit span as a function of θ according to the predictions of the first- and second-order regular perturbation theories of Section 3, the Galerkin solution as well as G_0 and $G_0 + \alpha G_1$ from this Section. The second-order regular perturbation is seen to be quite good up to about $\theta = 60°$ and then to deteriorate rapidly for larger angles of incidence. Both the first- and second-order regular perturbation results are useless for large angles of incidence while (16) is accurate in this region but not for moderate or small angles of incidence. The inclusion of the αG_1 term in (16) gives very little improvement over the simple approximation G_0. The most striking feature of Fig. 3 is that the wave force is not maximum at $\theta = 0°$ as might have been expected but rather at about $\theta = 55°$. This is hinted at by the second-order regular perturbation results and confirmed by the Galerkin results.

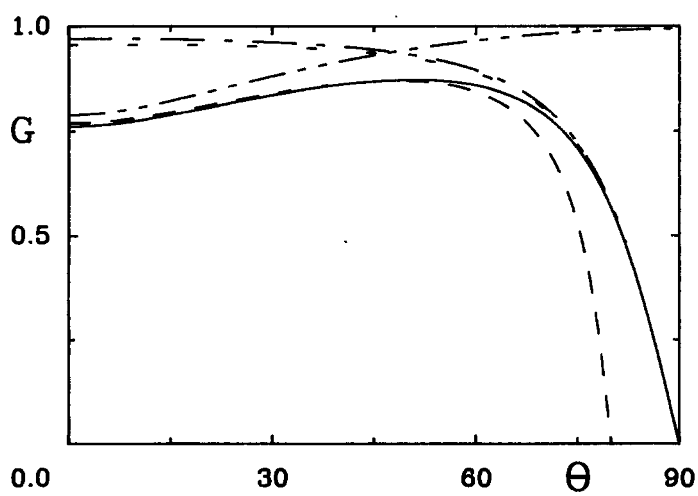

Fig. 3. The scaled, non-dimensional total normal wave force G for a planar outward-sloping sea wall $x = -\alpha y$ when $\omega = 2.0$ and $\alpha = 0.25$. We have shown the results of the Shanks-transformed Galerkin method (———) the first (—-·-—) and second (— — —) order regular perturbation theories as well as G_0 (-———-) and $G_0 + \alpha G_1$ (- - - - -) from (16).

5. Results and discussion

The perturbation solutions of Sections 3 and 4 were intended to provide a check on the Galerkin results and also to give some insight into the behaviour of the forces, such as that near $\theta = \pi/2$. For accurate numerical results, we use the Galerkin method supplemented by the use of the Shanks transform. In this section, we present representative results for low, intermediate and high frequency waves in the case where the wall is $x = -\alpha y$.

We begin with $\omega = 0.1$. In Fig. 4 we show the scaled total normal wave force per unit span G and its horizontal component H as functions of α for $\theta = 0°$ and $\theta = 75°$ for $0 \leqslant \alpha \leqslant 1.25$, the latter value of α being about the greatest for which reliable results could be obtained with the Shanks transform procedure. The curves for values of θ between 0° and 75° lie between the curves shown. In Fig. 5 we show G as a function of θ for $\alpha = 0.25$, $\alpha = 0.75$ and $\alpha = 1.25$. In this shallow-water case, it is clear that G is virtually independent of the angle of incidence except for very oblique waves and that the range of angles of incidence for which G is effectively constant increases as α decreases, i.e. as the wall becomes steeper. The normal force increases as α increases, except for extremely oblique waves. At normal incidence the horizontal component of the total force is seen to be virtually independent of α. This is in accord with the shallow-water theory solution discussed in [3]. At other angles of incidence the situation is very little different except for extremely obliquely incident waves. Thus, in shallow water, H is virtually independent of both θ and α except for θ near $\pi/2$.

In Figs. 6, 7 and 8 we show the corresponding results in water of intermediate depth, $\omega = 1.0$. The behaviour of the forces is now more complicated. At normal incidence, the total normal wave force G first increases with α but later decreases. At quite oblique incidence, it decreases monotonely with α. The horizontal component decreases with α for all θ. The range of angles of incidence for which G is effectively constant for fixed α is now very much reduced compared with the shallow-water case.

A deep-water case, $\omega = 3.0$, is shown in Figs. 9, 10 and 11. The largest useful value of α is now about 0.75. The normal and horizontal forces now decrease with α for all angles of incidence. However for fixed α they first increase as θ increases from 0, reach a maximum and

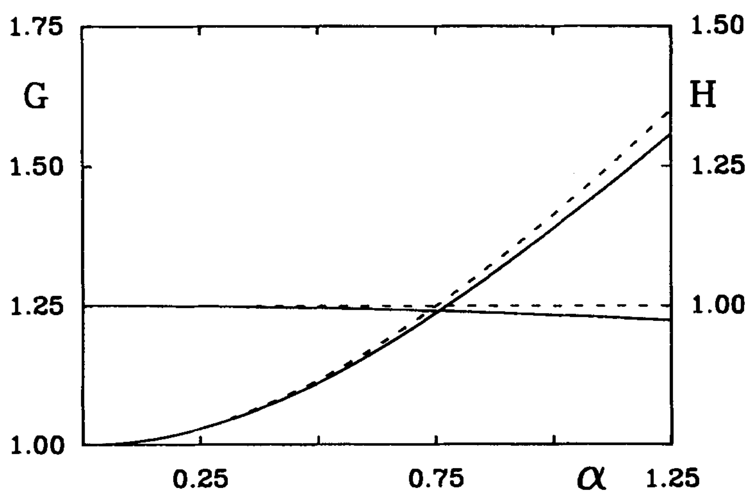

Fig. 4. The scaled, non-dimensional total normal, G, and horizontal, H, wave force according to the Shanks-transformed Galerkin method when $\omega = 0.1$ and hence $k^{-1} \tanh k = 0.99667$. The curves are for $\theta = 0°$ (- - - - - -) and $\theta° = 75°$ (———). The scale for G is on the left and that for H is on the right. These two quantities may be distinguished by the fact that H is virtually constant.

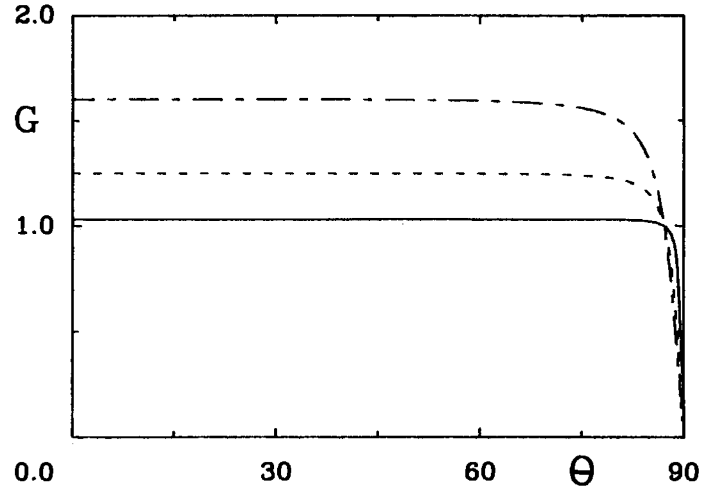

Fig. 5. As for Fig. 4 except that G is shown as a function of the angle of incidence θ (in degrees) for $\alpha = 0.25$ (———), $\alpha = 0.75$ (- - - - - -) and $\alpha = 1.25$ (- — - — -). The horizontal components may be found by dividing these by 1.03078, 1.25 and 1.60078 respectively.

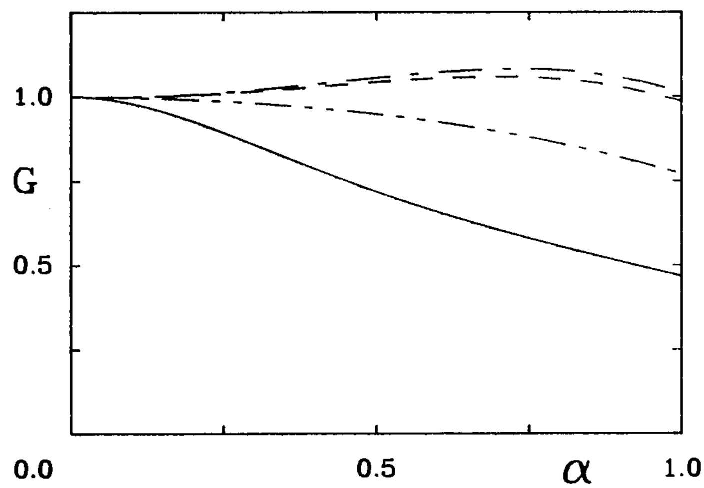

Fig. 6. As for Fig. 4 showing G, except that $\omega = 1.0$ and hence $k^{-1} \tanh k = 0.69482$. The four curves are for $\theta = 0°$ (- — - — -), $\theta = 30°$ (— — —), $\theta = 60°$ (— - - — - -) and $\theta = 75°$ (———).

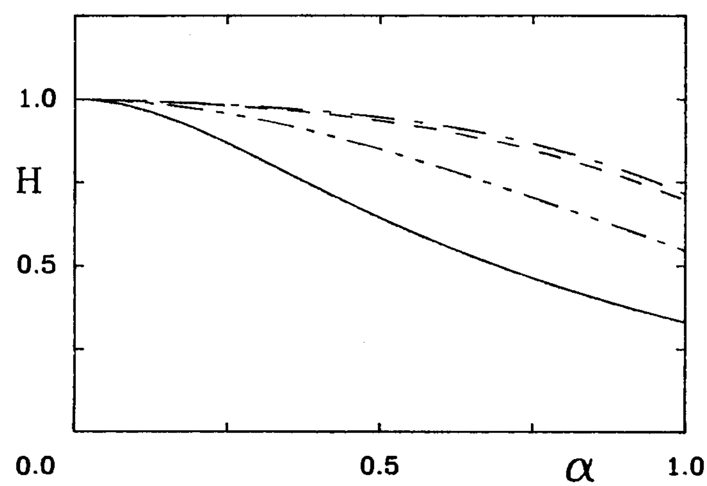

Fig. 7. As for Fig. 6, showing the horizontal component H of the total wave force per unit span.

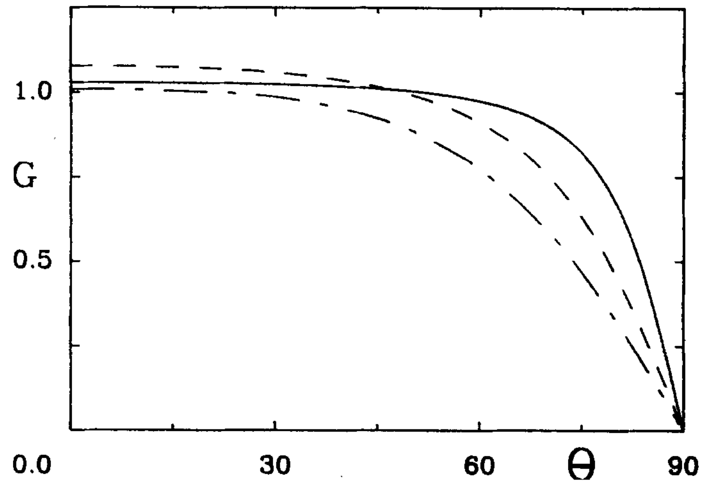

Fig. 8. As for Fig. 6, showing G as a function of θ for $\alpha = 0.35$ (———), $\alpha = 0.65$ (- - - - - -) and $\alpha = 1.0$ (- — - — -). The horizontal components may be found by dividing these by 1.05948, 1.19269 and 1.41421 respectively.

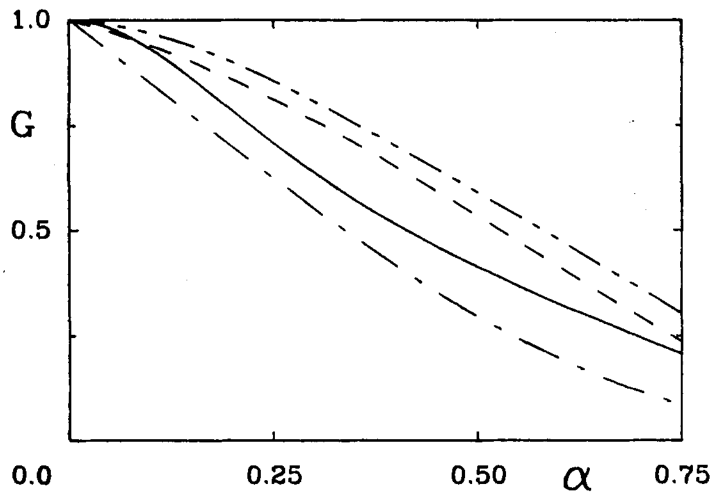

Fig. 9. As for Fig. 6 except that $\omega = 3.0$ and hence k^{-1} tanh $k = 0.11111$. The values of θ are the same as in Fig. 6.

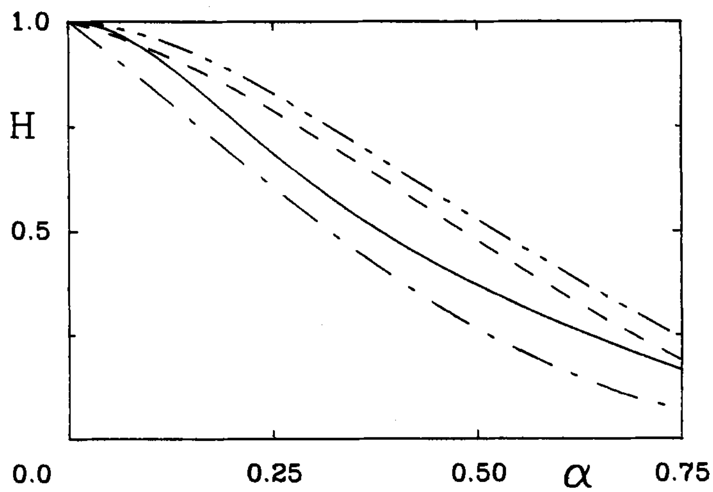

Fig. 10. As for Fig. 9, showing the horizontal component H.

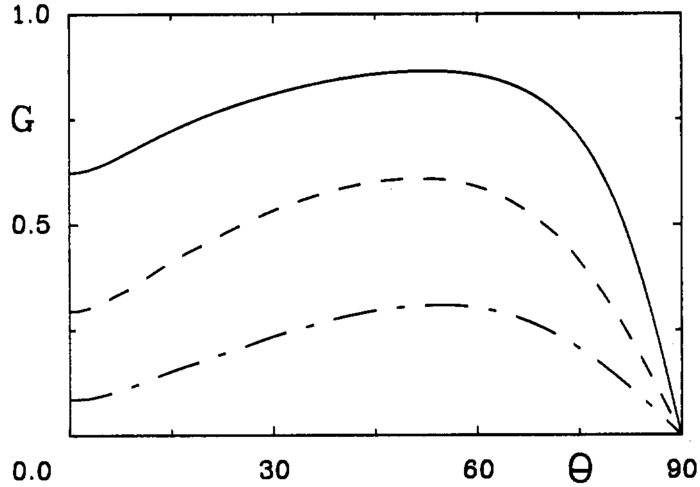

Fig. 11. As for Fig. 9, showing G as a function of θ for $\alpha = 0.25$ (———), $\alpha = 0.5$ (- - - - -) and $\alpha = 0.75$ (- — - —). The horizontal components may be found by dividing these by 1.03078, 1.11803 and 1.25 respectively.

then decrease to zero as $\theta \to \pi/2$. This unexpected feature is characteristic of short waves and was seen in Fig. 3.

To sum up: this paper has extended the work of [3] to the case of oblique incidence. With the exception of Section 4, the mathematics involved is a straightforward extension of that used in [3]. The major qualitative conclusions of [3], namely that the total normal wave force per unit span decreases as the wall steepens for shallow water but increases for deep water, has been found to be true also for oblique incidence, except for extremely obliquely incident waves. The fact that the force is not maximum at normal incidence in deep water is new and unexpected. The behaviour of extremely oblique waves is also a little unexpected. Provided the wall is not vertical they are reflected in such a way that the phase β is close to $\pi/2$ rather than 0. The boundary condition at $x = 0$ is effectively $\phi \approx 0$ rather than $\partial\phi/\partial x \approx 0$. The motion is therefore small near the wall and hence so are the forces. The situation when θ is exactly equal to $\pi/2$ is not covered by the work of this paper. In that case, the wave energy is travelling parallel to the wall and the type of solution employed here may not be appropriate since it may not be consistent to ignore the refraction of the waves over the sloping face of the wall. In any case refraction over off-shore depth contours would generally act to decrease the angle of incidence at which waves would hit the wall and so values of θ near $\pi/2$ are not likely to occur very often in practice. The situation for a real non-linear wave train is likely to be quite different from that discussed here for large angles of incidence. In that case, the reflection could be expected to be Mach reflection rather than the regular reflection assumed here. Some aspects of this type of reflection when the boundaries are vertical have been discussed by Yue and Mei [5].

Acknowledgements

This paper was written while the author was on leave at the University of Melbourne. He would like to thank the University of New South Wales for granting leave and the Chairman and staff of the Department of Mathematics at the University of Melbourne for their hospitality and the use of their computing facilities. Thanks are also due to an anonymous referee for suggesting some improvements to this paper, in particular the inclusion of the horizontal component of the force, and to A.J. Guttmann for discussions on extrapolation techniques.

References

1. J.D. Fenton: Wave forces on vertical walls, *J. Waterway, Port, Coastal and Ocean Engrg. ASCE* 111 (1985) 693–718.
2. L.W. Johnson and R.D. Riess: *Numerical analysis,* Addison Wesley, Reading, Mass., Second edn. (1982).
3. P.J. Kachoyan and W.D. McKee: Wave forces on steeply-sloping sea walls, *J. Engrg. Math.* 19 (1985) 351–362.
4. M. Van Dyke: *Perturbation methods in fluid mechanics,* Parabolic Press, Stanford, Calif. (1975).
5. D.K.P. Yue and C.C. Mei: Forward diffraction of Stokes waves by a thin wedge, *J. Fluid Mech.* 99 (1980) 33–52.